

Creep properties of (Si–Al–O–N)SiC whisker composites

TATSUYA SHIOGAI, KEIZOU TSUKAMOTO, NORIKAZU SASHIDA
Central Research Laboratory, Nihon Cement Co., Ltd, 1-2-23 Kiyosumi, Koto-ku, Tokyo 135, Japan

(Si–Al–O–N) (sialon)–SiC whisker (SiC_w) composites containing up to 10 mass% SiC_w were prepared by hot isostatic pressing. The strengths and the fracture toughness of composites remained relatively unchanged with the amount of SiC_w . The addition of SiC_w enabled us to improve the creep properties of sialon ceramics. The total creep strain and steady-state creep rate at 1473 K under a stress of 400–500 MPa decreased with increasing the amount of SiC_w . The experimental creep exponent values of monolithic sialon and sialon– SiC_w composites were nearly 1. It is supposed that the creep of both monolithic sialon and sialon– SiC_w composites are dominated by the viscous flow of the intergranular glassy phase. © 1998 Chapman & Hall

1. Introduction

Attempts have been made to use Si–Al–O–N (sialon) for high-temperature engineering materials because of its high strength, low thermal expansion coefficient and high oxidation resistance [1–5]. Recently some studies have been done on composites based on sialon to improve fracture toughness, creep resistance, fatigue properties, etc. [6–9].

Some work on SiC particle (SiC_p)–sialon composite [8, 10, 11] showed that the addition of SiC_p was effective in improving the high temperature strength and the creep resistance of sialon because of its fine microstructure. However, the fracture toughnesses of these composites were relatively low, because grains of sialon were made finer by the addition of SiC_p .

To improve the fracture toughness of sialon and silicon nitride, it is effective to elongate the grains of the sintered body [12–15]. On the other hand, the report of the present authors [16] showed that the fatigue parameter, n , of the toughened sialon ceramics with elongated grains was lower than sialon with fine grains and low fracture toughness.

The present authors [17] also reported that the addition of SiC whiskers (SiC_w) enabled the fatigue properties of sialon ceramics at room temperature to be improved.

The present work reports the effect of the addition of SiC_w to toughened sialon with elongated grains on creep properties.

2. Experimental procedure

2.1. Preparation of sialon– SiC_w composites

The raw materials of β -sialon with sintering aids are shown in Table I. The Si_3N_4 , AlN and Al_2O_3 contents correspond to β -sialon ($\text{Si}_{6-z}\text{Al}_2\text{O}_z\text{N}_{8-z}$) with $z = 0.3$.

Yttrium oxide and ytterbium oxide were added as densification additives. SiC_w (TWS-100, Tokai Carbon Co., Ltd, Japan; average diameter, 0.4 μm ; average length, 25 μm) dispersed with ethanol using an ultrasonic homogenizer, was added to the raw materials of β -sialon with sintering aids. The amounts of SiC_w added were 0, 5 and 10 mass%. The overall raw materials were mixed by ball milling with silicon nitride balls for 24 h in ethanol. Then, the slurry was dried under diminished pressure. The mixture was pressed in a die of 35 mm \times 50 mm under a pressure of 25 MPa. The compact was then pressed isostatically at 150 MPa. The pressed compacts were sintered at 2020 K for 6 h in a nitrogen atmosphere by pressureless sintering and then hot isostatically pressed at 1970 K for 3 h under a nitrogen pressure of 190 MPa.

2.2. Mechanical properties

The density of each specimen was measured by the Archimedes method. Young's modulus was measured by the resonance method. The sintered bodies were machined to rectangular bars of 3 mm \times 4 mm \times 40 mm for measurements of strength and fracture toughness. Four-point bending strength tests were conducted at a cross-head speed of 0.5 mm min⁻¹ with inner and outer spans of 10 mm and 30 mm, respectively. Bending tests were carried out in air at room temperature and 1473 K. The fracture toughness at room temperature was determined by the single-edge-pre-cracked-beam (SEPB) method.

2.3. Microstructure

The microstructures of sintered bodies were observed using scanning electron microscopy (SEM). The

TABLE I Raw materials of β -sialon

Material	Supplier	Amount (mass %)
α -Si ₃ N ₄	SN-E10, Ube Industries Ltd	89.8
AlN	F, Tokuyama Co., Ltd	3.4
Al ₂ O ₃	160-SG, Showa Denko K. K.	0.8
Y ₂ O ₃	Shin-Etsu Chemical Co., Ltd.	3.0
Yb ₂ O ₃	Shin-Etsu Chemical Co., Ltd.	3.0

specimens were polished and finished by the plasma etching technique [18] using CF₄ plasma.

2.4. Creep tests

Four-point flexural stress tests were conducted on lever-arm creep test machines. Flexural fixtures were SiC with inner and outer spans of 10 mm and 30 mm, respectively. Test bars were subjected to constant dead-weight loads at 1473 K in air. The creep measurement system includes an optical displacement detector. The strain was calculated from the measured flexural displacement assuming a constant radius of curvature between the inner load points.

3. Results and discussion

3.1. Mechanical properties and microstructure

Relative densities and Young's modulus of sintered bodies are plotted as a function of SiC_w content in Fig. 1. All specimens were fully densified, and Young's modulus slightly increased with increasing SiC_w content.

Bending strengths and fracture toughness values are plotted as a function of SiC_w content in Fig. 2. The strengths remained relatively unchanged with the amount of SiC_w. The strengths of sintered bodies at room temperature and at 1473 K were about 1100 MPa and 750 MPa, respectively. The fracture toughness of about 7.5 MPa m^{1/2} also remained relatively unchanged.

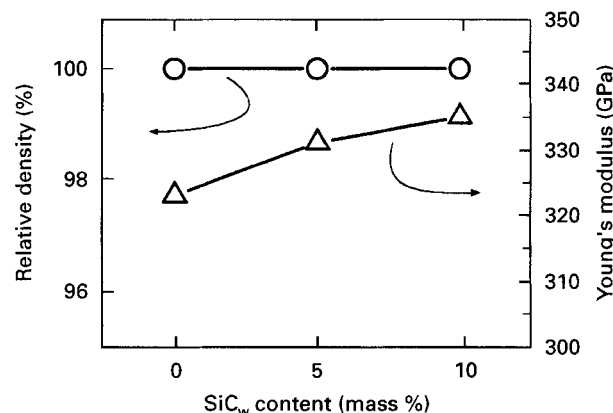


Figure 1 Relative density (○) and Young's modulus (△) of sintered sialons.

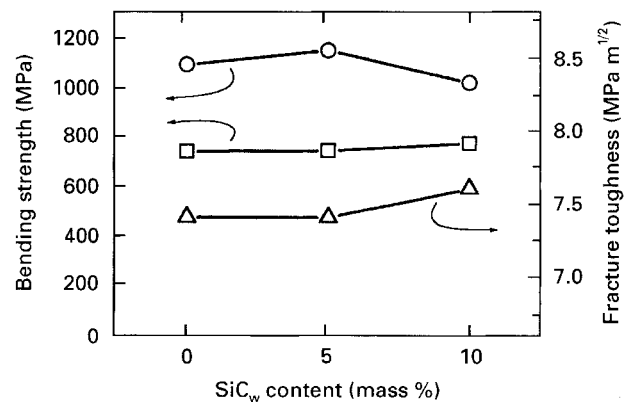


Figure 2 Bending strength at room temperature (○), bending strength at 1473 K (□) and fracture toughness (△) of sintered sialons.

Fig. 3 shows the SEM images of the sintered bodies. Surfaces were polished and finished by the plasma etching. The intergranular phase appears bright, and the grains appear dark. There is no significant difference between the sizes and the shapes of sialon grains in the specimens. All specimens contain elongated grains.

Some work on the SiC_p-sialon composite [8, 10, 11] showed that the addition of SiC_p inhibited the grain growth of sialon and the fracture toughnesses of the obtained composites were relatively low. However, in this work using up to 10 mass% SiC_w, the addition of SiC_w showed no inhibitory action against the grain growth of sialon matrix and the composite consequentially maintained a high fracture toughness.

3.2. Creep behaviour

Typical creep curves for monolithic sialon and composites containing SiC_w are shown in Fig. 4. The strain rate is also plotted in Fig. 4. There are no failures for the present testing time of 1.8×10^6 s. The final creep strain decreased with increasing amount of SiC_w under constant stresses of both 400 and 500 MPa. The creep rate decreased with increasing loading time and showed an almost constant value after testing each specimen for about 1.5×10^6 s.

Fig. 5 shows the relationship between applied stress and minimum (steady-state) creep rate. The minimum creep rate decreased with increasing SiC_w content. The straight lines in Fig. 5 are obtained by the least-squares method. All experimental data points are approximately on the straight lines. The estimated creep exponent from the slope of the regression lines are 1.1 for monolithic sialon, 1.2 for the composite containing 5 mass% SiC_w and 1.3 for the composite with 10 mass% SiC_w.

In silicon nitride or sialon with an intergranular glassy phase, the experimentally creep exponent value is often obtained to be 2 [19]. In that case, it is suggested that the mechanism of creep is intergranular slip with formation of a cavity [19, 20]. On the other hand, when the creep is dominated by the viscous flow

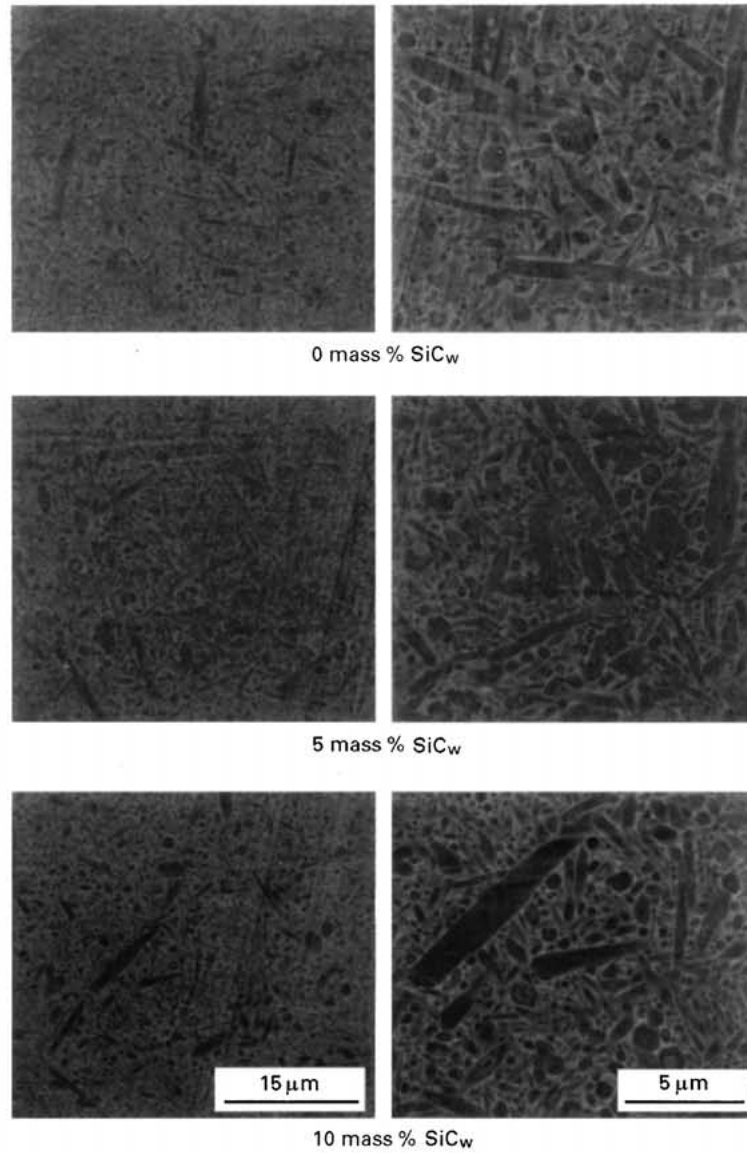


Figure 3 Scanning electron micrographs of sintered sialons. Surfaces were polished and finished by plasma etching technique.

of intergranular glassy phase, the strain rate, $d\varepsilon/dt$, follows [21]

$$\frac{d\varepsilon}{dt} = A\sigma \frac{(W/D)^3}{\eta} \quad (1)$$

where A is a constant, σ is the applied stress, W is the thickness of the intergranular glassy phase, D is the grain size and η is the viscosity coefficient of the intergranular phase.

In the present work, creep exponent values were nearly 1:4, it is supposed that the creep of both monolithic sialon and sialon-SiC_w composites are dominated by the viscous flow of the intergranular glassy phase. Therefore, with increasing amount of SiC_w, the mechanism of creep remains unchanged and only the creep resistance increased.

It is considered that the reasons for improvement in the creep properties are the thinning of the intergranular glassy phase by the dispersion and the bridging effect of SiC_w.

4. Conclusions

Sialon-SiC_w composites containing up to 10 mass% SiC_w were prepared by hot isostatic pressing. The effect of the addition of SiC_w to toughened sialon with elongated grains on creep properties were investigated. The results obtained were as follows.

1. The strengths and the fracture toughness of composites remained relatively unchanged with the amount of SiC_w.

2. The addition of SiC_w enabled us to improve the creep properties of sialon ceramics. The total creep strain and steady state creep rate at 1473 K under a stress of 400–500 MPa decreased with increasing amount of SiC_w.

3. It is supposed that the creep of both monolithic sialon and sialon-SiC_w composites is dominated by the viscous flow of intergranular glassy phase, because experimental creep exponent values were nearly 1.

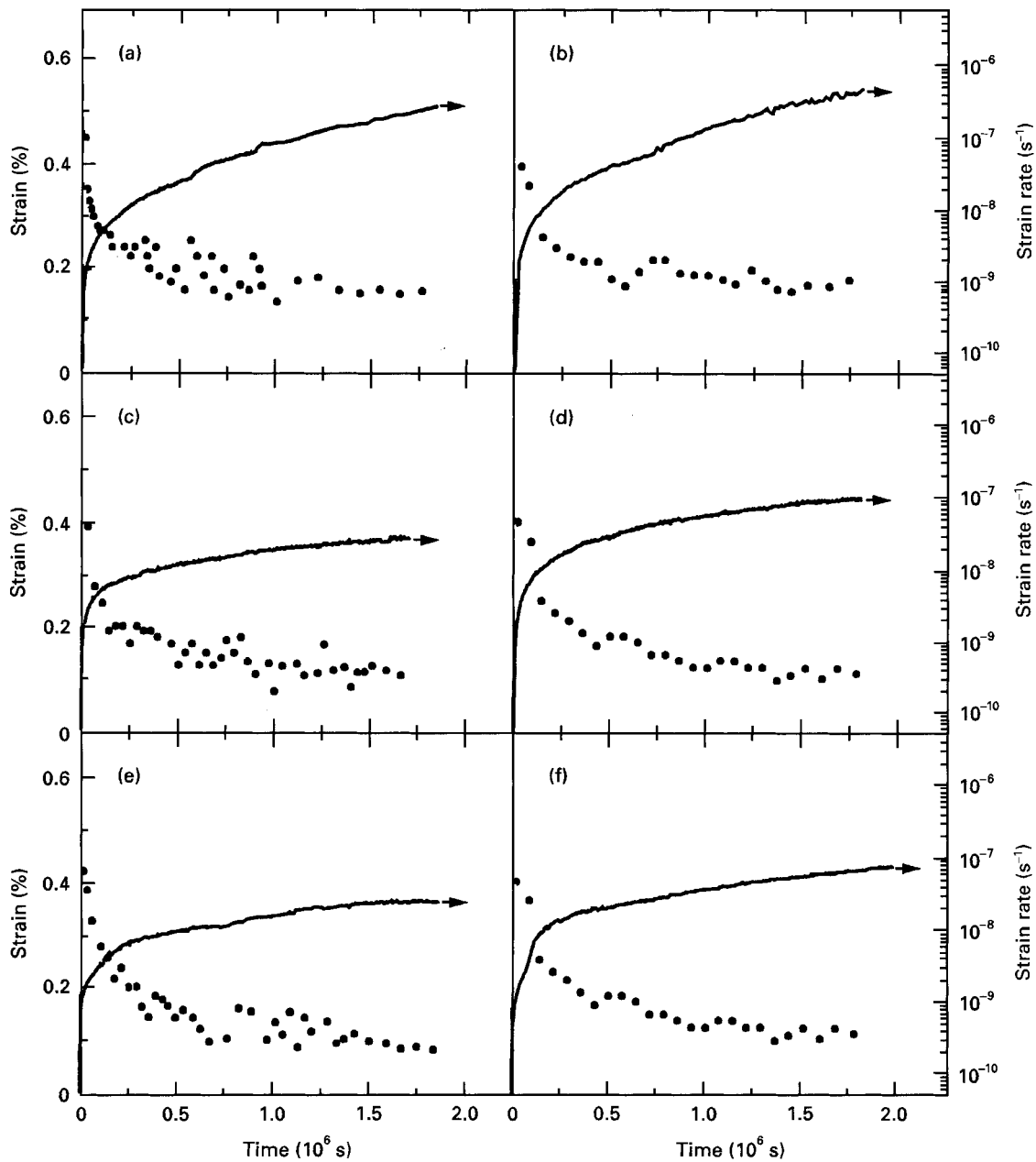


Figure 4 Creep curves, i.e., strain (—), and strain rates (●) of sintered sialons: (a) 0 mass% SiC_w, 400 MPa; (b) 0 mass% SiC_w, 500 MPa; (c) 5 mass% SiC_w, 400 MPa; (d) 5 mass% SiC_w, 500 MPa; (e) 10 mass% SiC_w, 400 MPa; (f) 10 mass% SiC_w, 500 MPa.

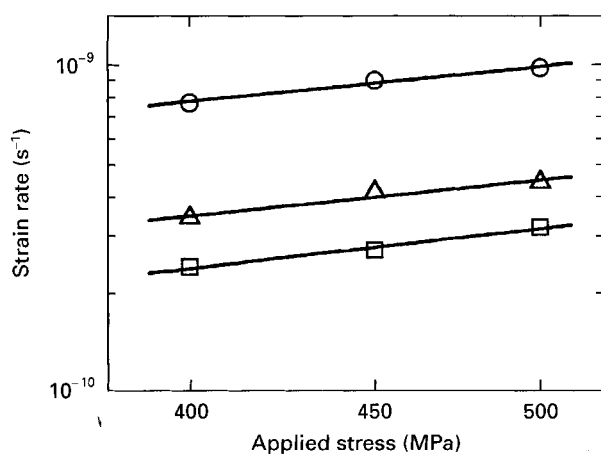


Figure 5 Stress dependence of minimum creep rate. The estimated creep exponent was 1.1 for monolithic sialon (○), 1.2 for 5 mass% SiC_w (△) and 1.3 for 10 mass% SiC_w (□).

Acknowledgement

This work is a part of the Automotive Ceramics Gas Turbine Development Program conducted by the Petroleum Energy Center of Japan.

References

1. K. H. JACK, *J. Mater. Sci.* **11** (1976) 1135.
2. Y. OYAMA and O. KAMIGAITO, *Yogyo Kyokai Shi* **80** (1972) 327.
3. M. MITOMO, N. KURAMOTO and Y. INOMATA, *J. Mater. Sci.* **14** (1979) 2309.
4. M. MITOMO, N. KURAMOTO, Y. INOMATA and M. TSUTSUMI, *Yogyo Kyokai Shi*, **88** (1980) 489.
5. Y. HASEGAWA, M. MITOMO, K. HIROTA, H. TANAKA, Y. FUJII and H. SUZUKI, *ibid.* **89** (1981) 533.
6. A. TSUGE, K. NISHIDA and M. KOMATSU, *J. Amer. Ceram. Soc.* **58** (1975) 323.

7. C. YAMAGISHI, K. TSUKAMOTO, J. HAKOSHIMA and Y. AKIYAMA, *J. Mater. Sci.* **27** (1992) 1908.
8. C. YAMAGISHI, K. MINAMISAWA, T. SHIOGAI and K. SUZUKI, *J. Jpn. Soc. Powder and Powder Metall.* **39** (1992) 1113.
9. Y. AKIMUNE, *J. Mater. Sci. Lett.* **9** (1990) 816.
10. T. SHIOGAI, K. MINAMISAWA, M. HAYASHI, C. YAMAGISHI, K. TSUKAMOTO and E. YASUDA, *J. Jpn. Soc. Powder Powder Metall.* **41** (1994) 835.
11. T. SHIOGAI, K. MINAMISAWA, M. HAYASHI, C. YAMAGISHI, K. TSUKAMOTO and E. YASUDA, *ibid.* **41** (1994) 839.
12. F. F. LANGE, *J. Amer. Ceram. Soc.* **62** (1979) 428.
13. E. TANI, S. UMEBAYASHI, K. KISHI, K. KOBAYASHI and M. NISHIJIMA, *Amer. Ceram. Soc. Bull.* **65** (1986) 1311.
14. T. KAWASHIMA, H. OKAMOTO, H. YAMAMOTO and A. KITAMURA, *Seramikkusu Ronbunshi* **99** (1991) 320.
15. N. HIROSAKI, M. ANDO, Y. AKIMUNE and M. MITOMO, *J. Ceram. Soc. Jpn.* **100** (1992) 1366.
16. T. SHIOGAI, N. MIYATA, N. SASHIDA, K. TSUKAMOTO, E. YASUDA, *ibid.* **104** (1996) 562.
17. T. SHIOGAI, N. SASHIDA, K. TSUKAMOTO, *ibid.* **104** (1996) 760.
18. M. MITOMO, Y. SATO, N. AYUZAWA and I. YASHIMA, *J. Amer. Ceram. Soc.* **74** (1991) 856.
19. W. R. CANNON and T. G. LANGDON, *J. Mater. Sci.* **18** (1983) 1.
20. A. G. EVANS and A. RANA, *Acta Metall.* **28** (1983) 129.
21. G. M. PHARR and M. F. ASHBY, *ibid.* **31** (1983) 129.

*Received 24 June
and accepted 20 August 1996*